RESEARCH LETTER

Growth media and temperature effects on biofilm formation by serotype O157:H7 and non-O157 Shiga toxin-producing *Escherichia coli*

Gaylen A. Uhlich, Chin-Yi Chen, Bryan J. Cottrell & Ly-Huong Nguyen

Molecular Characterization of Foodborne Pathogens Research Unit, Eastern Regional Research Center, Agricultural Research Service, U.S. Department of Agriculture, Wyndmoor, PA, USA

Correspondence: Gaylen A. Uhlich, Molecular Characterization of Foodborne Pathogens Research Unit, Eastern Regional Research Center, Agricultural Research Service, U.S. Department of Agriculture, 600 East Mermaid Lane, Wyndmoor, PA 19038-8542, USA. Tel.: 215 233 6740; fax: 215 233 6581; e-mail: gaylen.uhlich@ars.usda.gov

Received 11 December 2013; revised 8 February 2014; accepted 1 April 2014. Final version published online 22 April 2014.

DOI: 10.1111/1574-6968.12439

Editor: David Clarke

Keywords
STEC; serotype O157:H7; biofilm; temperature regulation; Congo red.

Abstract

Biofilm formation in most *Escherichia coli* strains is dependent on curli fimbriae and cellulose, and the production of both varies widely among pathogenic strains. Curli and cellulose production by colonies growing on agar are often identified by their affinity for Congo red dye (CR). However, media composition and incubation temperature can affect dye affinity and impose limitations on red phenotype detection by this method. In this study, we compared different Shiga toxin-producing *E. coli* for CR affinity and biofilm formation under different media/temperature conditions. We found strain and serotype differences in CR affinities and biofilm formation, as well as temperature and media requirements for maximum CR binding. We also constructed strains with deletions of curli and/or cellulose genes to determine their contributions to the phenotypes and identified two O45 strains with a medium-dependent induction of cellulose.

Introduction

Escherichia coli biofilm formation typically requires the production of adhesive curli fimbriae and the exopolysaccharide, cellulose (Olsén *et al.*, 1989; Zogaj *et al.*, 2001). Curli are encoded by *csgBA*, and cellulose production is directed from the *bcsABZC* gene cluster in which *bcsA* (cellulose synthase) and *bcsC* are essential (Römling *et al.*, 1998; Zogaj *et al.*, 2001). Cellulose and curli are often identified using their affinity for Congo red (CR) dye. In certain *Salmonella* and *E. coli*, growth on agar containing CR produces a brown colony when producing curli, a pink phenotype when producing cellulose, and a dark red and dry phenotype when producing both (Zogaj *et al.*, 2001; Solano *et al.*, 2002). Strains producing neither remain white. Cellulose is also detected by its affinity for calcofluor, which produces fluorescence under a UV light source (Zogaj *et al.*, 2001; Solano *et al.*, 2002). In a study of commensal *E. coli*, biofilm formation was strongest among strains that produced both cellulose and curli and reduced in strains producing only one factor (Bokranz *et al.*, 2005). A few strains formed some biofilm in the absence of both. Curli and cellulose expression requires the transcriptional regulator CsgD. CsgD directly activates the curli structural operon, *csgBAC*, and indirectly stimulates cellulose expression by increasing *adrA* transcription. The diguanylate cyclase activity of AdrA produces cyclic(c) di-GMP that is essential for cellulose production (Gerstel & Römling, 2003; Barnhart & Chapman, 2006). CsgD regulation is complex requiring protein transcription factors, GGDEF/EAL proteins that control c-di-GMP levels, and various sRNAs (Gerstel & Römling, 2003; Sommerfeldt *et al.*, 2009; Ogasawara *et al.*, 2010a, b; Thomason & Storz, 2010; Jørgensen *et al.*, 2012). Such regulation allows *csgD* transcription to respond to extracellular stimuli such as osmolarity, pH, O_2 concentrations, catabolite levels, and membrane alterations (Vidal *et al.*, 1998; Gerstel & Römling, 2001; Jack-

FEMS MICROBIOLOGY LETTERS

son *et al.*, 2002; Ferrières & Clarke, 2003; Dorel *et al.*, 2006; Ogasawara *et al.*, 2007). Strain and/or serotype differences in *csgD* expression would be expected due to the high number of regulators and the complexity of the network. We previously showed that Shiga toxin-producing *E. coli* (STEC) varied greatly in their ability to express curli and generate biofilm (Chen *et al.*, 2013; Uhlich *et al.*, 2013). Curli and biofilm deficiencies in serotype O157:H7 likely stem from bacteriophage insertions in *mlrA*, a DNA-binding protein that enhances RpoS-driven *csgD* transcription (Uhlich *et al.*, 2013). In non-O157:H7 STEC, strong biofilm formation was more readily observed. The lowest expression was seen in strains with motility deficiencies, RpoS mutations, or prophage insertions in *mlrA* (Chen *et al.*, 2013). These studies were performed using Congo red indicator (CRI) agar for CR affinity studies (Hammar *et al.*, 1996), Luria–Bertani (LB) broth with no salt (LB-NS) to maximize biofilm expression (Uhlich *et al.*, 2006), and 23–25 °C incubations to simulate environmental conditions. However, other STEC studies have described CR-binding differences dependent on temperature and culture media (Saldaña *et al.*, 2009). In this study, we compared CR affinity and biofilm formation under different media/temperature conditions. In addition, we tested strains with deletions of curli and/or cellulose genes to determine their contributions to the phenotypes observed.

Materials and methods

Bacterial strains and mutant construction

Bacterial strains are listed in Table 1. Non-O157:H7 isolates from the seven important serogroups (O26, O45, O103, O111, O113, O121, and O145) were prescreened to include strains with a range of biofilm phenotypes (Chen *et al.*, 2013). Strain 43894OR (OR), a constitutive curli-producing strain, was used as a positive control for biofilm and Congo red (CR) dye affinity studies (Uhlich *et al.*, 2001). Strain 43895 (43895OW in certain previous studies), shown to be a nonbiofilm-forming isolate on different surfaces in various media, was used as a negative biofilm control (Uhlich *et al.*, 2006, 2013). Cultures from frozen glycerol stocks were recovered on LB agar at 30 °C. When appropriate, kanamycin (25 mg L^{-1}) and chloramphenicol (10 mg L^{-1}) were added. Gene deletions were constructed by replacing the ORF with a neomycin resistance cassette (neo) as previously described (Uhlich, 2009); *csgBA* deletions removed sequence from the *csgB* start codon to the *csgA* stop codon. All deletions in the FCL1 strain were generated using a chloramphenicol resistance cassette (Gene Bridges GmbH). The *csgB* gene in strains PA5 and PA46, and *csgA* in strain SJ7 were deleted instead of *csgBA*; *bcsC* was deleted in strain SJ7. Deletions were verified by PCR, and resistance cassettes were not cured.

CR affinity, biofilm, and cellulose assays

CR affinity was assayed on CRI or T-medium agar (Collinson *et al.*, 1991) containing 20 mg L^{-1} CR dye and 10 mg L^{-1} Coomassie brilliant blue G-250 (TA). Calcofluor (Fluorescent brightener 28; Sigma) was added to T-medium agar at 200 mg L^{-1} to detect cellulose (Uhlich *et al.*, 2006). Biofilm was assayed as previously described using YESCA broth (medium base for CRI) and T-medium at 25 and 30 °C; selected strains were tested at 37 °C (Hammar *et al.*, 1996; Uhlich *et al.*, 2013). The mean optical densities at 590 nm ($OD_{590\ nm}$) of eluted crystal

Table 1. Strains used in this study

Strain	Serotype	Source*	Reference
E. coli			
PA1-PA52	O157:H7	PADH	Hartzell *et al.* (2011)
43895	O157:H7	ATCC	Hamburger isolate, 1982
43894OR	O157:H7	Laboratory collection	Uhlich *et al.* (2001)
06F00475	O157:H7	PADH	Uhlich *et al.* (2008)
B6-914	O157:H7	ATCC	Beutin *et al.* (1989)
FCL1	O103:H2	Mexico	Chen *et al.* (2013)
DA-33	O103:H2	MSU	Medina *et al.* (2012)
SJ10	O103:H2	CDC	Medina *et al.* (2012)
SJ14	O111:H8	CDC	Medina *et al.* (2012)
98-8338	O111:NM	PHAC	Medina *et al.* (2012)
SJ13	O111:NM	CDC	Medina *et al.* (2012)
SJ15	O113: NT†	CDC	Chen *et al.* (2013)
SJ29	O113:H21	CDC	Medina *et al.* (2012)
04-1450	O113:H21	PHAC	Fratamico & Bagi (2012)
DEC10	O26:H11	MSU	Medina *et al.* (2012)
05-6544	O26:H11	PHAC	Medina *et al.* (2012)
05-6545	O45:H2	PHAC	Medina *et al.* (2012)
96-3285	O45:H2	PHAC	Medina *et al.* (2012)
SJ7	O45:H2	CDC	Medina *et al.* (2012)
SJ16	O121:H19	CDC	Medina *et al.* (2012)
SJ18	O121:H19	CDC	Medina *et al.* (2012)
03-4064	O121:NM	PHAC	Medina *et al.* (2012)
SJ24	O145:NM	CDC	Medina *et al.* (2012)
E59	O145:H28	ARS	Wasilenko *et al.* (2012)
Salmonella enterica			
3934	Enteritidis		Uhlich *et al.* (2006)
942	Enteritidis		Uhlich *et al.* (2006)
1170/97	Enteritidis		Uhlich *et al.* (2006)

*ARS, Agricultural Research Service, Eastern Regional Research Center; ATCC, American Type Culture Collection, Manassas, VA, USA; CDC, US Centers for Disease Control and Prevention, Atlanta, Georgia, USA; MSU, Michigan State University Department of Microbiology and Molecular Genetics STEC Center, East Lansing, Michigan, USA; PADH, Pennsylvania Department of Health; PHAC, Public Health Agency of Canada, Winnipeg, Manitoba, Canada.
†NT: flagellar antigen typing was not performed.

violet (CV) from four wells of each strain were calculated. At temperatures of 25 and 30 °C, the means of all strains, calculated for a particular media type, were compared with control strain 43895 using a Dunnett's test. Strains with mean OD values significantly greater ($P < 0.05$) than strain 43895 were interpreted as having developed biofilm. Their frequencies at 25 and 30 °C in YESCA broth and T-medium were subjected to logistical regression, and odds ratios were calculated for parameters showing a significant effect (SAS/STAT 9.3, Cary, NC).

Results

Medium and temperature effects on CR affinity in serotype O157:H7 STEC

Strain appearance on CRI and TA after 48-h incubation at different temperatures is shown in Fig. 1. Light reflection off the dry surface of strain OR masked its underlying color in many images, but its true red color is apparent at the colony borders, particularly on TA at 25 and 30 °C (Fig. 1a). There was little CR binding by the O157:H7 strains on CRI at 25 °C with only PA32 and PA46 showing red color. At 30 °C, PA32 and PA46 became darker red and most other strains appeared pale brown. At 37 °C, most strains showed elevated brown color. PA6 and PA46 were the only strains showing dark red staining. Strain PA1 was noteworthy in being the only strain whose red color intensity diminished with each temperature increase. In strain PA32, red color was most intense at 30 °C but diminished at 37 °C. In general, color was darker on TA than CRI. At 25 °C, PA32 and PA46 stained the darkest red, but strains such as PA1, PA51, and B6-914 also showed low CR affinity. Some additional strains showed red coloring on TA at 30 °C, but PA32 and PA46 remained the darkest.

Many O157:H7 strains showed more intense red staining on TA at 37 °C than at 30 °C, but a few strains (PA32, PA1, PA7, PA52, and B6-914) stained less at 37 °C than at 30 °C, indicating that the optimal temperature for CR binding varies among strains. It should be noted that few strains showed dark red staining under optimal conditions, none had a dry appearance, and only strains PA46 (at 30 and 37 °C) and PA32 (at 30 °C)

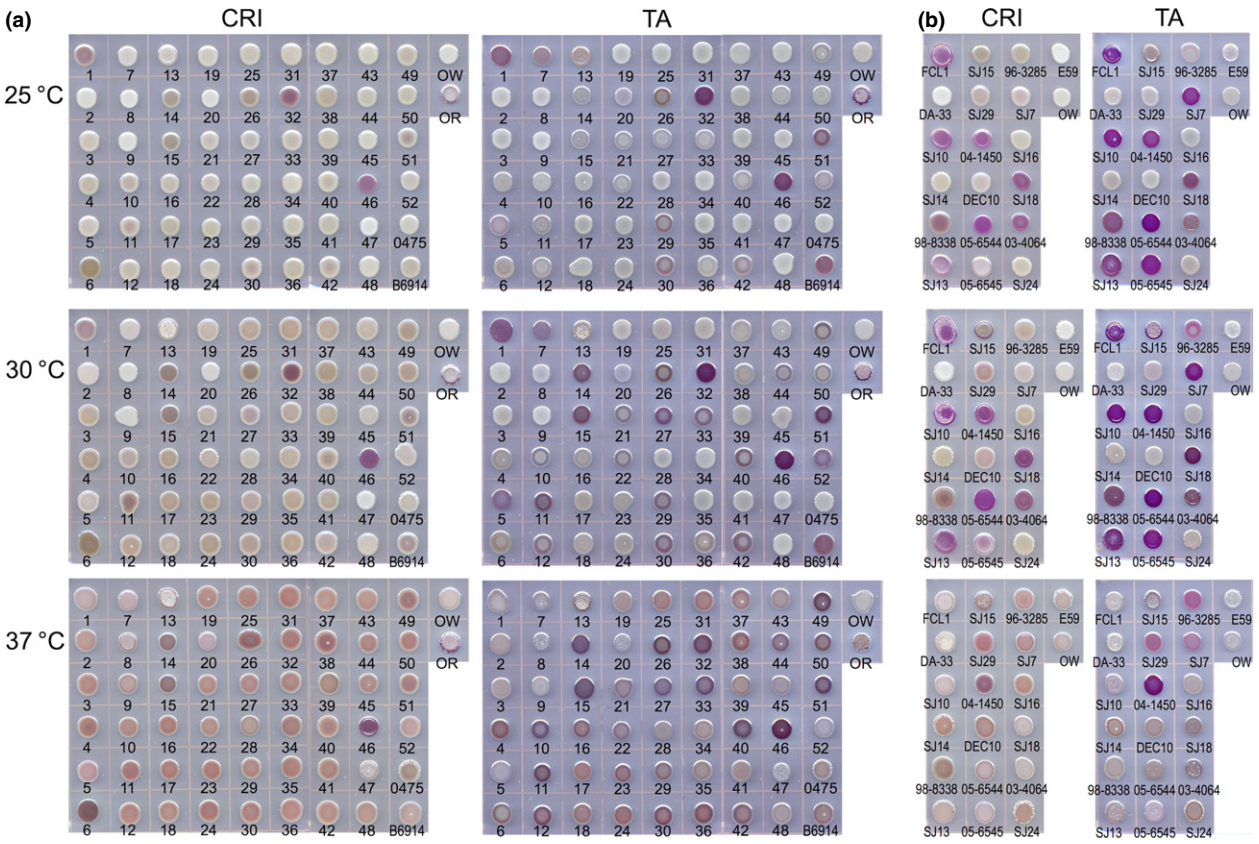

Fig. 1. Congo red affinity of (a) serotype O157:H7 strains and (b) non-O157:H7 STEC strains spotted on CRI agar or TA and incubated at 25 °C, 30 °C, and 37 °C for 48 h. Pennsylvania O157:H7 isolates are designated by number without the 'PA' prefix; OW, 43895; OR, 43894OR; 0475, 06F00475.

showed red color comparable with the 43894OR control. Even under more favorable media and temperature conditions, CR affinity in serotype O157:H7 is relatively low.

Medium and temperature effects on CR affinity in non-O157:H7 STEC

When tested on CRI, eight non-O157:H7 STEC strains showed red color but none approached the color intensity of strain OR at 25 °C (Fig. 1b). At 37 °C, there was a dramatic reduction in color (six strains lost nearly all CR affinity) and the dry phenotype (FCL1, SJ10, and SJ13). Only strain 04-1450 showed dark staining, which was relatively consistent at all three temperatures. The results of non-O157:H7 STEC on TA was overall similar to those seen on CRI, except that the intensity was increased and the color of some strains possessed a purple hue. In contrast to the O157:H7 strains, CR affinity was repressed at 37 °C on both CRI and TA in those non-O157 STEC strains capable of strong CR binding, except for strain 04-1450 whose color remained strong at all three temperatures. Strains SJ29 and 96-3285 showed enhanced CR binding at 30 and 37 °C but not at 25 °C. Similar to the O157:H7 strains, TA enhanced CR affinity compared with that displayed on CRI, but it did not affect CR affinity in strains that showed little or no affinity on CRI. Strains SJ7 and 05-6545 were exceptions, showing strong color on TA but little color on CRI.

Curli- and cellulose-defective mutants

Deletions in the *csg* or *bcs* operons were constructed in selected CR-binding strains to study the role of curli and cellulose in CR affinity (Fig. 2). For the O157:H7 strains, *csgBA* deletion resulted in complete loss of CR affinity, indicating an essential role for curli. Deletion of *bcs*A had little effect on CR affinity in these strains.

For non-O157:H7 mutant strains, CR binding was more evident at 25 °C than 37 °C. While *bcs* deletion resulted in either no effect or complete loss of CR affinity, depending on strain background, deletion of the *csgB/A* genes resulted in reduction in CR affinity and changes in hue, from purple to pink. Deletion of *csgD*, the essential regulator of both curli and cellulose, completely abolished CR affinity in all non-O157 strains tested.

For SJ7 and 05-6545 (previously shown to be curli-deficient on CRI; Chen *et al.*, 2013), which showed CR affinity on TA but not on CRI, deletion of *bcs* genes eliminated CR affinity at 25 °C, indicating that cellulose was responsible for CR binding. However, deletion of *csg* genes reduced CR affinity, suggesting that a low level of curli expression may augment CR binding by cellulose in those strains. This concurs with earlier findings where extracellular curli production by strain 05-6545 could be detected by anti-CsgA antibodies but not by protein staining (Chen *et al.*, 2013). Interestingly, at 37 °C where most CR affinity of the non-O157 strains was repressed, deletion of *csgBA* allowed greater CR affinity in strain 05-6545.

At 25 °C, curli-producing strains 05-6544 and FCL1 (Chen *et al.*, 2013) showed complete loss of red staining when *csgD* was deleted and partial loss when *csgBA* was deleted, indicating that curli and cellulose were both required for full CR affinity. However, *bcsA* deletion had little effect on strain color, suggesting that cellulose either played a very minor role or its contributions were masked by strong curli expression. At 37 °C, CR affinity was low on both media for all four non-O157:H7 parent

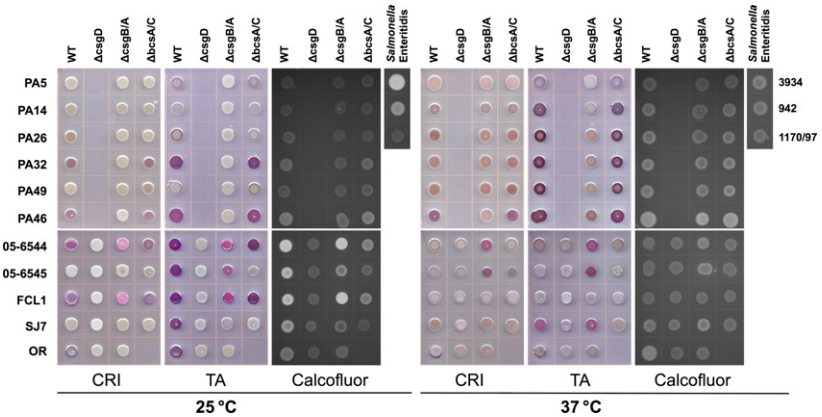

Fig. 2. Congo red affinity and calcofluor binding of selected serotype O157:H7 strains (top panels) and non-O157:H7 STEC strains (bottom panels) and their isogenic mutants spotted on CRI agar, TA, or T-medium + calcofluor and incubated at 25 and 37 °C for 48 h. Fluorescence was viewed using a 365 nm UV transilluminator. ΔcsgB/A, deletion of either *csgBA, csgB, or csgA*; ΔbcsA/C, deletion of either *bcsA* or *bcsC*; OR, 43894OR. Control strains for calcofluor binding: *S.* Enteritidis 3934 (cellulose positive; curli positive), 942 (cellulose negative; curli positive), and 1170/97 (cellulose negative; curli negative).

strains. However, deletion of *csgBA* genes enhanced CR binding in strain 05-6544 and 05-6545 on both media. It was not clear why the suppression of CR binding in certain non-O157 STEC strains was reversed by *csg* deletions at 37 °C.

Calcofluor staining for cellulose production

Calcofluor binding of select strains is also shown in Fig. 2. Calcofluor binding was minimal in O157:H7 strains with no difference in staining between *bcsA* mutants and parents at any temperature, indicating that cellulose was not expressed. A barely discernible fluorescence reduction between *csgBA* mutants and the PA32 and PA46 parents suggests a slight calcofluor affinity for curli in those strains, as is apparent in the *Salmonella* Enteritidis control strain 942 (curli+, cellulose−).

All non-O157 parent strains tested showed some fluorescence at 25 °C. Deletion of *bcsA* and *csgD* reduced the fluorescence, indicating that cellulose is binding calcofluor. There were no differences between the *bcsA* mutants and parents of the non-O157 strains at 37 °C. However, *csgBA* deletion caused a slight fluorescence increase in some strains, suggesting that curli may interfere with calcofluor binding by other cellular components. At 25 °C, *csgD* deletion eliminated all calcofluor affinity in the non-O157:H7 parent strains. Deletion of *csgBA* in 05-6544 and FCL1 did not affect the intense fluorescence of the parents; however, *bcsA* deletion severely decreased the intensity, indicating that cellulose was responsible for most calcofluor binding. The residual staining in *bcsA* mutants likely represents minor binding by either curli or a different CsgD-regulated factor. We also tested SJ7 and 05-6545 on calcofluor-containing CRI-base medium at 25 °C and found no fluorescence (results not shown). Considering the differences in color on CRI/TA and in fluorescence by calcofluor staining of the mutants and parents, we believe that the dark purple color (more apparent on TA) was due to curli binding, while the pink/magenta color was mostly attributed to cellulose binding.

Biofilm formation on polystyrene

Biofilm formation was tested using both YESCA broth and T-medium at 25 and 30 °C; a subset of strains was also tested at 37 °C (Table 2). None of the serotype O157:H7 strains formed significant amounts of biofilm using YESCA at 25 °C including PA32 and PA46, the two strains that bound CR on CRI at 25 °C. Using T-medium at 25 °C, only strain PA46 ($OD_{590\ nm}$ = 0.69) and PA7 ($OD_{590\ nm}$ = 0.19) formed significant biofilm. When cultured at 30 °C, PA46 formed biofilm in both YESCA broth ($OD_{590\ nm}$ = 0.22) and T-medium ($OD_{590\ nm}$ = 0.82). Strains PA14, PA15, and PA32 also formed small amounts of biofilm using T-medium ($OD_{590\ nm}$ = 0.15–0.24). We also tested biofilm formation at 37 °C in 12 O157:H7 strains that showed higher CR affinities. Of the 12 strains, only PA46 formed trace amounts of stainable biofilm (CV $OD_{590\ nm}$ = 0.18) in T-medium. Although 37 °C appears favorable for serotype O157:H7 CR affinity, it was the poorest of the three temperatures for supporting biofilm formation.

The non-O157 STEC were better biofilm formers than the O157:H7 strains at 25 and 30 °C, but they formed little biofilm at 37 °C (Table 2). Most strains that bound CR dye also tended to form biofilm; however, CR dye-binding intensity did not necessarily correspond with the amount of biofilm formation. There was considerable strain variation regarding the optimum temperature and medium for biofilm formation. Strains 05-6545 and SJ14 bound CR poorly on CRI but formed low to moderate biofilm on both media at 25 and 30 °C. Strains 98-8338, SJ15, SJ7, and 03-4064 bound visible amounts of CR dye under most conditions but generated little or no biofilm. Therefore, CR binding had limited value for predicting biofilm formation on polystyrene in individual strains.

Logistic regression analysis revealed a significant medium effect on biofilm formation with strains being 2.69 times more likely to form biofilms in T-medium compared with YESCA broth. There was no significant effect determined for temperature between 25 and 30 °C.

Discussion

In this study, we compared non-O157 STEC from seven important O-serogroups to serotype O157:H7 strains for growth media and temperature effects on CR affinity and biofilm formation. Both O157:H7 and non-O157 STEC showed higher CR affinity on TA than on CRI. Comparison of curli isolations from selected strains grown on TA and CRI showed greater curli protein production on TA, indicating that CR binding increases were due to higher curli production rather than increased CR-binding efficiency (data not shown). This agrees with previous findings (Saldaña *et al.*, 2009). We also showed that CR binding by O157:H7 strains was usually greater at 30 and 37 °C than at 25 °C. However, the optimal temperature varied among strains. In contrast, the non-O157 STEC tended to prefer 25 and 30 °C, and most strains showed little CR binding at 37 °C. Such findings suggest that certain adhesion factors have become more adapted for usage at host temperatures in O157:H7 strains than in other STEC. However, studies with more strains from each non-O157:H7 serogroup will be needed to buttress this conclusion.

Table 2. 48-h biofilm formation on polystyrene in T-medium broth and YESCA broth at 25 °C

		CV $OD_{590\ nm}$ ± SD† at 25 °C		CV $OD_{590\ nm}$ ± SD† at 30 °C		CV $OD_{590\ nm}$ ± SD† at 37 °C	
Strain	Serotype	YESCA	T-medium	YESCA	T-medium	YESCA	T-medium
43894OR	O157:H7	2.54 ± 0.053‡	1.39 ± 0.060‡	2.42 ± 0.132‡	1.22 ± 0.079‡	1.43 ± 0.115	1.34 ± 0.056
43895	O157:H7	0.13 ± 0.009	0.09 ± 0.008	0.08 ± 0.005	0.07 ± 0.004	ND	ND
PA1	O157:H7	0.09 ± 0.002	0.13 ± 0.012	0.11 ± 0.004	0.09 ± 0.005	ND	ND
PA2	O157:H7	0.10 ± 0.008	0.09 ± 0.004	0.08 ± 0.003	0.08 ± 0.002	ND	ND
PA3	O157:H7	0.08 ± 0.005	0.09 ± 0.004	0.09 ± 0.002	0.08 ± 0.001	ND	ND
PA4	O157:H7	0.10 ± 0.010	0.09 ± 0.002	0.08 ± 0.004	0.08 ± 0.003	ND	ND
PA5	O157:H7	0.11 ± 0.003	0.11 ± 0.004	0.09 ± 0.004	0.10 ± 0.007	ND	ND
PA6	O157:H7	0.07 ± 0.004	0.08 ± 0.005	0.07 ± 0.002	0.07 ± 0.005	0.08 ± 0.003	0.08 ± 0.003
PA7	O157:H7	0.09 ± 0.003	0.19 ± 0.031*	0.08 ± 0.005	0.14 ± 0.027	0.07 ± 0.002	0.07 ± 0.002
PA8	O157:H7	0.09 ± 0.006	0.09 ± 0.004	0.08 ± 0.004	0.09 ± 0.002	ND	ND
PA9	O157:H7	0.09 ± 0.005	0.11 ± 0.006	0.08 ± 0.006	0.08 ± 0.003	ND	ND
PA10	O157:H7	0.09 ± 0.008	0.10 ± 0.005	0.09 ± 0.002	0.09 ± 0.004	ND	ND
PA11	O157:H7	0.12 ± 0.009	0.09 ± 0.004	0.11 ± 0.018	0.11 ± 0.006	ND	ND
PA12	O157:H7	0.09 ± 0.006	0.11 ± 0.011	0.09 ± 0.006	0.09 ± 0.005	ND	ND
PA13	O157:H7	0.07 ± 0.008	0.10 ± 0.008	0.09 ± 0.012	0.09 ± 0.003	ND	ND
PA14	O157:H7	0.09 ± 0.007	0.12 ± 0.006	0.10 ± 0.003	0.24 ± 0.080*	0.07 ± 0.001	0.08 ± 0.003
PA15	O157:H7	0.08 ± 0.004	0.11 ± 0.006	0.09 ± 0.004	0.20 ± 0.065*	0.07 ± 0.005	0.08 ± 0.001
PA16	O157:H7	0.10 ± 0.005	0.10 ± 0.014	0.09 ± 0.001	0.08 ± 0.005	ND	ND
PA17	O157:H7	0.10 ± 0.002	0.10 ± 0.006	0.01 ± 0.007	0.08 ± 0.005	ND	ND
PA18	O157:H7	0.10 ± 0.004	0.10 ± 0.004	0.01 ± 0.003	0.08 ± 0.002	ND	ND
PA19	O157:H7	0.09 ± 0.003	0.10 ± 0.003	0.09 ± 0.004	0.08 ± 0.003	ND	ND
PA20	O157:H7	0.09 ± 0.007	0.15 ± 0.019	0.09 ± 0.006	0.11 ± 0.013	ND	ND
PA21	O157:H7	0.11 ± 0.003	0.11 ± 0.005	0.08 ± 0.004	0.09 ± 0.002	ND	ND
PA22	O157:H7	0.09 ± 0.004	0.10 ± 0.005	0.07 ± 0.003	0.08 ± 0.003	ND	ND
PA23	O157:H7	0.09 ± 0.001	0.07 ± 0.003	0.07 ± 0.006	0.08 ± 0.004	ND	ND
PA24	O157:H7	0.10 ± 0.002	0.07 ± 0.002	0.08 ± 0.010	0.08 ± 0.003	ND	ND
PA25	O157:H7	0.09 ± 0.007	0.07 ± 0.002	0.08 ± 0.004	0.07 ± 0.004	ND	ND
PA26	O157:H7	0.09 ± 0.007	0.07 ± 0.003	0.08 ± 0.004	0.08 ± 0.006	0.08 ± 0.003	0.08 ± 0.003
PA27	O157:H7	0.10 ± 0.007	0.08 ± 0.003	0.09 ± 0.004	0.01 ± 0.010	0.08 ± 0.004	0.08 ± 0.005
PA28	O157:H7	0.10 ± 0.010	0.08 ± 0.002	0.08 ± 0.005	0.08 ± 0.004	ND	ND
PA29	O157:H7	0.12 ± 0.004	0.09 ± 0.003	0.09 ± 0.004	0.09 ± 0.006	ND	ND
PA30	O157:H7	0.12 ± 0.006	0.07 ± 0.003	0.08 ± 0.006	0.08 ± 0.004	ND	ND
PA31	O157:H7	0.10 ± 0.005	0.08 ± 0.003	0.07 ± 0.005	0.08 ± 0.003	ND	ND
PA32	O157:H7	0.08 ± 0.001	0.11 ± 0.012	0.10 ± 0.002	0.15 ± 0.009*	0.07 ± 0.002	0.08 ± 0.004
PA33	O157:H7	0.10 ± 0.007	0.08 ± 0.005	0.09 ± 0.005	0.10 ± 0.006	0.07 ± 0.005	0.08 ± 0.004
PA34	O157:H7	0.10 ± 0.011	0.08 ± 0.002	0.08 ± 0.005	0.08 ± 0.004	ND	ND
PA35	O157:H7	0.10 ± 0.009	0.08 ± 0.003	0.08 ± 0.004	0.08 ± 0.003	ND	ND
PA36	O157:H7	0.12 ± 0.009	0.08 ± 0.003	0.08 ± 0.003	0.09 ± 0.002	0.08 ± 0.005	0.09 ± 0.014
PA37	O157:H7	0.11 ± 0.015	0.08 ± 0.004	0.08 ± 0.001	0.08 ± 0.004	ND	ND
PA38	O157:H7	0.08 ± 0.003	0.09 ± 0.008	0.11 ± 0.006	0.09 ± 0.007	ND	ND
PA39	O157:H7	0.10 ± 0.010	0.07 ± 0.002	0.08 ± 0.005	0.07 ± 0.002	ND	ND
PA40	O157:H7	0.10 ± 0.004	0.09 ± 0.006	0.08 ± 0.003	0.10 ± 0.006	ND	ND
PA41	O157:H7	0.09 ± 0.003	0.08 ± 0.001	0.09 ± 0.006	0.08 ± 0.006	ND	ND
PA42	O157:H7	0.11 ± 0.009	0.07 ± 0.002	0.09 ± 0.002	0.08 ± 0.001	ND	ND
PA43	O157:H7	0.11 ± 0.010	0.08 ± 0.004	0.09 ± 0.004	0.08 ± 0.004	ND	ND
PA44	O157:H7	0.11 ± 0.005	0.08 ± 0.003	0.08 ± 0.002	0.08 ± 0.005	ND	ND
PA45	O157:H7	0.09 ± 0.004	0.09 ± 0.003	0.10 ± 0.004	0.09 ± 0.009	ND	ND
PA46	O157:H7	0.12 ± 0.005	0.69 ± 0.085*	0.22 ± 0.038*	0.82 ± 0.197*	0.10 ± 0.003	0.18 ± 0.109
PA47	O157:H7	0.08 ± 0.003	0.08 ± 0.003	0.09 ± 0.004	0.08 ± 0.003	ND	ND
PA48	O157:H7	0.08 ± 0.004	0.08 ± 0.004	0.09 ± 0.006	0.08 ± 0.005	ND	ND
PA49	O157:H7	0.10 ± 0.006	0.09 ± 0.004	0.11 ± 0.022	0.09 ± 0.007	0.07 ± 0.004	0.08 ± 0.004
PA50	O157:H7	0.08 ± 0.005	0.08 ± 0.003	0.09 ± 0.006	0.09 ± 0.006	ND	ND
PA51	O157:H7	0.09 ± 0.008	0.09 ± 0.005	0.09 ± 0.010	0.09 ± 0.003	0.08 ± 0.002	0.08 ± 0.005
PA52	O157:H7	0.11 ± 0.004	0.13 ± 0.008	0.09 ± 0.005	0.11 ± 0.006	ND	ND

Table 2. Continued

Strain	Serotype	CV $OD_{590\ nm}$ ± SD† at 25 °C		CV $OD_{590\ nm}$ ± SD† at 30 °C		CV $OD_{590\ nm}$ ± SD† at 37 °C	
		YESCA	T-medium	YESCA	T-medium	YESCA	T-medium
06F00475	O157:H7	0.08 ± 0.006	0.08 ± 0.002	0.07 ± 0.004	0.08 ± 0.005	ND	ND
B6-914	O157:H7	0.08 ± 0.004	0.10 ± 0.009	0.06 ± 0.004	0.08 ± 0.005	ND	ND
FCL1	O103:H2	0.62 ± 0.105*	1.63 ± 0.105*	0.69 ± 0.221*	1.16 ± 0.021*	0.08 ± 0.004	0.08 ± 0.003
DA-33	O103:H2	0.14 ± 0.013	0.09 ± 0.003	0.10 ± 0.005	0.08 ± 0.004	ND	ND
SJ10	O103:H2	1.98 ± 0.447*	1.61 ± 0.133*	1.77 ± 0.009*	0.72 ± 0.176*	0.07 ± 0.003	0.07 ± 0.002
SJ14	O111:H8	0.17 ± 0.019	0.40 ± 0.027*	0.25 ± 0.004*	0.57 ± 0.011*	ND	ND
98-8338	O111:NM	0.08 ± 0.004	0.12 ± 0.012	0.06 ± 0.003	0.07 ± 0.007	0.07 ± 0.003	0.07 ± 0.003
SJ13	O111:NM	0.27 ± 0.007*	0.66 ± 0.102*	0.11 ± 0.011	0.17 ± 0.028*	0.07 ± 0.001	0.08 ± 0.006
SJ15	O113:NT	0.08 ± 0.005	0.10 ± 0.004	0.07 ± 0.002	0.07 ± 0.004	ND	ND
SJ29	O113:H21	0.08 ± 0.003	0.08 ± 0.006	0.07 ± 0.004	0.07 ± 0.002	0.08 ± 0.004	0.08 ± 0.005
04-1450	O113:H21	0.26 ± 0.017*	1.31 ± 0.104*	0.63 ± 0.039*	1.30 ± 0.104*	ND	ND
DEC10	O26:H11	0.10 ± 0.004	0.08 ± 0.005	0.08 ± 0.004	0.07 ± 0.003	ND	ND
05-6544	O26:H11	0.21 ± 0.012	1.73 ± 0.035*	0.48 ± 0.034*	0.80 ± 0.022*	ND	ND
05-6545	O45:H2	0.53 ± 0.051*	1.39 ± 0.120*	0.70 ± 0.039*	0.85 ± 0.018*	ND	ND
96-3285	O45:H2	0.09 ± 0.006	0.09 ± 0.003	0.08 ± 0.005	0.10 ± 0.007	ND	ND
SJ7	O45:H2	0.10 ± 0.004	0.30 ± 0.036*	0.07 ± 0.003	0.08 ± 0.003	ND	ND
SJ16	O121:H19	0.09 ± 0.004	0.09 ± 0.003	0.08 ± 0.007	0.08 ± 0.003	ND	ND
SJ18	O121:H19	0.48 ± 0.034*	0.69 ± 0.100*	0.12 ± 0.004	0.51 ± 0.004*	0.07 ± 0.002	0.08 ± 0.003
03-4064	O121:NM	0.13 ± 0.010	0.18 ± 0.015*	0.08 ± 0.006	0.23 ± 0.023*	ND	ND
SJ24	O145:NM	0.11 ± 0.068	0.08 ± 0.005	0.07 ± 0.002	0.07 ± 0.003	ND	ND
E59	O145:H28	0.09 ± 0.004	0.08 ± 0.005	0.07 ± 0.002	0.08 ± 0.002	ND	ND
Media control		0.09 ± 0.004	0.10 ± 0.013	0.09 ± 0.004	0.09 ± 0.012	0.08 ± 0.003	0.08 ± 0.002

†Values represent the mean optical density (OD) ± standard deviation (SD) measured at 590 nm of crystal violet (CV) dye eluted from four stained wells/sample. The experimental means calculated for each of the strains using the designated medium at either 25 °C or 30 °C were compared with that of control strain 43895 under the same conditions using the Dunnett's Test.

‡Strain 43894OR was not included in the analysis.

*Strain mean different ($P = 0.05$) from the control strain 43895.

In addition to temperature and media differences, variations in cellulose production were also identified. Serotype O157:H7 strains showed little cellulose production and complete dependence on curli for CR binding at each temperature and media combination tested. On the other hand, mutational analyses of a small number of non-O157:H7 STEC strains demonstrated that both cellulose and curli played a role in CR binding. It was unclear why serotype O157:H7 strains failed to produce cellulose and whether such failures resulted in optimum temperature differences or lowered CR affinities compared with most non-O157 STEC. Previously, we determined that a high incidence of prophage insertions in *mlrA* and heterogeneous *rpoS* mutations limited *csgD*-dependent phenotypes in O157:H7 strains (Uhlich *et al.*, 2013). Decreased cellulose expression may be an additional consequence. However, curli production at 37 °C could also imply utilization of a different sigma factor at higher incubation temperatures. It remains to be seen whether *rpoD* replaces *rpoS* at higher temperatures, altering *csgD* dependence on *mlrA* and establishing a different regulatory pathway for both cellulose and curli production. We also identified O45:H2 strains showing a medium-dependent, differential expression of cellulose that resulted in CR and calcofluor binding on TA but not on CRI. This was likely due to substrate utilization differences. We are currently conducting experiments to identify the components involved.

At 30 °C, a few native O157:H7 strains bound CR and formed small amounts of biofilm, but at 37 °C where CR affinity was greatest, biofilm was not formed, except for the traces by PA46. In contrast to the native strains, control strain OR, which overexpresses *csgD* from a mutant promoter, produced high levels of biofilm at all temperatures. It is possible that differences in curli expression alone may have resulted in the drastic biofilm differences between the native strains and strain OR at 37 °C, given that hyperexpression of a regulatory factor from a mutant promoter may cause unique phenotypic presentations. However, it is unclear why native strains with low curli expression at 30 °C produced more biofilm than the same native strains producing even more curli at 37 °C. Clearly, other factors besides curli production contributed to the differential biofilm phenotypes. Our studies showing no *bcsA/C*-dependent calcofluor staining of the serotype O157:H7 strains at either temperature indicate that cellulose did not contribute to the biofilm differences in these strains.

Unlike the O157:H7 strains, many non-O157 strains produced abundant biofilms. Cellulose and curli both

affected CR binding, but there was significant individual strain variation in the phenotypic consequences of curli and/or cellulose gene deletions, especially at various temperatures. Gualdi *et al.* (2008) found that cellulose and curli expression had variable effects on biofilm formation in a nonpathogenic *E. coli* strain. Low curli-expressing strain MG1655 was made biofilm proficient by overexpressing plasmid-encoded *csgD*. Cellulose was suppressed at 37 °C but expressed at 30 °C due to temperature-regulated *adrA* expression. Biofilm formation was suppressed at 30 °C when cellulose blocked curli adhesion, but was generated at 37 °C when cellulose was absent. In the absence of curli expression, cellulose acted as a weak adhesin, indicating that cellulose can both promote or repress biofilm formation, depending on the level of curli expression. Clearly, the regulation of curli and cellulose, their roles in biofilm formation, and their interactions postexpression are complex and contribute to high phenotypic variability among strains. More studies will be needed to understand their role in the STEC.

In this study, we defined certain media and temperature effects on CR affinity and biofilm formation that will aid in defining the optimum conditions for identifying these characteristics in different clinically important STEC strains. In addition, we described differences in cellulose production among STEC serotypes and identified serogroup O45 STEC strains with medium-dependent cellulose production. This study also indicates that the CR-binding phenotype may be a reasonable predictor of ambient-temperature biofilm formation in strains of serotype O157:H7, whose cellulose production is low. However, in certain other STEC serogroups, co-expression of curli and cellulose at different levels leads to high phenotypic variability that may confound the correlation between curli expression and biofilm formation.

Acknowledgements

We thank John Phillips (ARS, USDA) for assistance with statistical analyses and Carlos Gamazo (University of Navarra, Navarra, Spain) for the gift of *Salmonella* Enteritidis strains 3934, 942, and 1170/97.

Author's contribution

G.A. Uhlich and C.-Y. Chen contributed equally to this report.

Disclaimer

USDA is an equal opportunity provider and employer. Mention of trade names or commercial products in this article is solely for the purpose of providing specific information and does not imply recommendation or endorsement by the U.S. Department of Agriculture.

References

Barnhart MM & Chapman MR (2006) Curli biogenesis and function. *Annu Rev Microbiol* **60**: 131–147.

Beutin L, Montenegro MA, Orskov I, Orskov F, Prada J, Zimmermann S & Stephan R (1989) Close association of verotoxin (Shiga-like toxin) production with enterohemolysin production in strains of *Escherichia coli*. *J Clin Microbiol* **27**: 2559–2564.

Bokranz W, Wang X, Tschäpe H & Römling U (2005) Expression of cellulose and curli fimbriae by *Escherichia coli* isolated from the gastrointestinal tract. *J Clin Microbiol* **54**: 1171–1182.

Chen CY, Hofmann CS, Cottrell BJ, Strobaugh TP Jr, Paoli GC, Nguyen LH, Yan X & Uhlich GA (2013) Phenotypic and genotypic characterization of biofilm forming capabilities in non-O157 Shiga toxin-producing *Escherichia coli* strains. *PLoS ONE* **8**: e84863.

Collinson SK, Emödy L, Müller KH, Trust TJ & Kay WW (1991) Purification and characterization of thin, aggregative fimbriae from *Salmonella enteritidis*. *J Bacteriol* **173**: 4773–4781.

Dorel C, Lejeune P & Rodrigue A (2006) The Cpx system of *Escherichia coli*, a strategic signaling pathway for confronting adverse conditions and for settling biofilm communities? *Res Microbiol* **157**: 306–314.

Ferrières L & Clarke DJ (2003) The RcsC sensor kinase is required for normal biofilm formation in *Escherichia coli* K-12 and controls the expression of a regulon in response to growth on a solid surface. *Mol Microbiol* **50**: 1665–1682.

Fratamico PM & Bagi LK (2012) Detection of Shiga toxin-producing *Escherichia coli* in ground beef using the GeneDisc real-time PCR system. *Front Cell Infect Microbiol* **2**: 152.

Gerstel U & Römling U (2001) Oxygen tension and nutrient starvation are major signals that regulate *agfD* promoter activity and expression of the multicellular morphotype in *Salmonella typhimurium*. *Environ Microbiol* **3**: 638–648.

Gerstel U & Römling U (2003) The *csgD* promoter, a control unit for biofilm formation in *Salmonella typhimurium*. *Res Microbiol* **154**: 659–667.

Gualdi L, Tagliabue L, Bertagnoli S, Ieranò T, De Castro C & Landini P (2008) Cellulose modulates biofilm formation by counteracting curli-mediated colonization of solid surfaces in *Escherichia coli*. *Microbiology* **154**: 2017–2024.

Hammar M, Bian Z & Normark S (1996) Nucleator-dependent intercellular assembly of adhesive curli organelles in *Escherichia coli*. *P Natl Acad Sci USA* **93**: 6562–6566.

Hartzell A, Chen C, Lewis C, Liu K, Reynolds S & Dudley EG (2011) *Escherichia coli* O157:H7 of genotype lineage-specific polymorphism assay 211111 and clade 8 are common clinical isolates within Pennsylvania. *Foodborne Pathog Dis* **8**: 763–768.

Jackson DW, Simecka JW & Romeo T (2002) Catabolite repression of *Escherichia coli* biofilm formation. *J Bacteriol* **184**: 3406–3410.

Jørgensen MG, Nielsen JS, Boysen A, Franch T, Møller-Jensen J & Valentin-Hansen P (2012) Small regulatory RNAs control the multi-cellular adhesive lifestyle of *Escherichia coli*. *Mol Microbiol* **84**: 36–50.

Medina MB, Shelver WL, Fratamico PM, Fortis L, Tillman G, Narang N, Cray WC Jr, Esteban E & Debroy A (2012) Latex agglutination assays for detection of non-O157 Shiga toxin-producing *Escherichia coli* serogroups O26, O45, O103, O111, O121, and O145. *J Food Prot* **75**: 819–826.

Ogasawara H, Hasegawa A, Kanda E, Miki T, Yamamoto K & Ishihama A (2007) Genomic SELEX search for target promoters under the control of the PhoQP-RstBA signal relay cascade. *J Bacteriol* **189**: 4791–4799.

Ogasawara H, Yamamoto K & Ishihama A (2010a) Regulatory role of MlrA in transcription activation of *csgD*, the master regulator of biofilm formation in *Escherichia coli*. *FEMS Microbiol Lett* **312**: 160–168.

Ogasawara H, Yamada K, Kori A, Yamamoto K & Ishihama A (2010b) Regulation of *Escherichia coli csgD* promoter: interplay between five transcription factors. *Microbiology* **156**: 2470–2483.

Olsén A, Jonsson A & Normark S (1989) Fibronectin binding mediated by a novel class of surface organelles on *Escherichia coli*. *Nature* **338**: 652–655.

Römling U, Bian Z, Hammar M, Sierralta WD & Normark S (1998) Curli fibers are highly conserved between *Salmonella typhimurium* and *Escherichia coli* with respect to operon structure and regulation. *J Bacteriol* **180**: 722–731.

Saldaña Z, Xicohtencati-Cortes J, Avelino F, Phillips AD, Kaper JB, Puente JL & Girón JA (2009) Synergistic role of curli and cellulose in cell adherence and biofilm formation of attaching and effacing *Escherichia coli* and identification of Fis as a negative regulator of curli. *Environ Microbiol* **11**: 992–1006.

Solano C, Garcia B, Valle J, Berasain C, Ghigo J-M, Gamazo C & Lasa L (2002) Genetic analysis of *Salmonella enteritidis* biofilm formation: critical role of cellulose. *Mol Microbiol* **43**: 793–808.

Sommerfeldt N, Possling A, Becker G, Pesavento C, Tschowri N & Hengge R (2009) Gene expression patterns and differential input into curli fimbriae regulation of all GGDEF/EAL domain proteins in *Escherichia coli*. *Microbiology* **155**: 1318–1331.

Thomason MK & Storz G (2010) Bacterial antisense RNAs: how many are there, and what are they doing? *Annu Rev Genet* **44**: 167–188.

Uhlich GA (2009) KatP contributes to OxyR-regulated hydrogen peroxide resistance in *Escherichia coli* serotype O157:H7. *Microbiology* **155**: 3589–3598.

Uhlich GA, Keen JE & Elder RO (2001) Mutations in the *csgD* promoter associated with variations in curli expression in certain strains of *Escherichia coli* O157:H7. *Appl Environ Microbiol* **67**: 2367–2370.

Uhlich GA, Cooke PH & Solomon EB (2006) Analyses of the red-dry-rough phenotype of an *Escherichia coli* O157:H7 strain and its role in biofilm formation and resistance to antibacterial agents. *Appl Environ Microbiol* **72**: 2564–2572.

Uhlich GA, Sinclair JR, Warren NG, Chmielecki WA & Fratamico P (2008) Characterization of Shiga toxin-producing *Escherichia coli* isolates associated with two multistate food-borne outbreaks that occurred in 2006. *Appl Environ Microbiol* **74**: 1268–1272.

Uhlich GA, Chen CY, Cottrell BJ, Hofmann CS, Dudley EG, Strobaugh TP Jr & Nguyen LH (2013) Phage insertion in *mlrA* and variations in *rpoS* limit curli expression and biofilm formation in *Escherichia coli* serotype O157:H7. *Microbiology* **159**: 1586–1596.

Vidal O, Longin R, Prigent-Combaret C, Dorel C, Hooreman M & Lejeune P (1998) Isolation of an *Escherichia coli* K-12 mutant strain able to form biofilms on inert surfaces: involvement of a new *ompR* allele that increases curli expression. *J Bacteriol* **180**: 2442–2449.

Wasilenko JL, Fratamico PM, Narang N, Tillman GE, Ladely S, Simmons M & Cray WC Jr (2012) Influence of primer sequences and DNA extraction method on detection of non-O157 Shiga toxin-producing *Escherichia coli* in ground beef by real-time PCR targeting the *eae*, *stx*, and serogroup-specific genes. *J Food Prot* **75**: 1939–1950.

Zogaj X, Nimtz M, Rohde M, Bokranz W & Römling U (2001) The multicellular morphotypes of *Salmonella typhimurium* and *Escherichia coli* produce cellulose as the second component of the extracellular matrix. *Mol Microbiol* **39**: 1452–1463.